REPORT DOCUMENTATION PAG

AFRL-SR-BL-TR-98

0470

)proved
)704-0188

1. AGENCY USE ONLY (*Leave Blank*)	2. REPORT DATE	3. REPORT TYPE AND DATES COVERED
	May 20, 1998	Final Report 2/15/94--2/14/98

4. TITLE AND SUBTITLE
Large Eddy and Unstructured Grid Methods for Heat Transfer Applications in Propulsion Systems

5. FUNDING NUMBERS
AFOSR Grant F49620-94-1-0168

6. AUTHORS
Richard H. Pletcher

7. PERFORMING ORGANIZATION NAME(S) AND ADDRESS(ES)
Department of Mechanical Engineering
Black Engineering Building
Iowa State University
Ames, Iowa 50011

8. PERFORMING ORGANIZATION REPORT NUMBER
ISU-ERI-Ames-98405

9. SPONSORING / MONITORING AGENCY NAME(S) AND ADDRESS(ES)
Air Force Office of Scientific Research /NA
Turbulence and Internal Flows
110 Duncan Ave, Suite B115
Bolling Air Force Base, D.C, 20332-0001

10. SPONSORING / MONITORING AGENCY REPORT NUMBER

11. SUPPLEMENTARY NOTES

12a. DISTRIBUTION / AVAILABILITY STATEMENT
Distribution Statement A. Approved for public release; distribution is unlimited.

12b. DISTRIBUTION CODE

13. ABSTRACT *(Maximum 200 words)*

Large eddy simulation methods have been developed to compute compressible turbulent flows with heat transfer. The formulation employs preconditioning to permit efficient use in the low Mach number regime. Efficient algorithms have been developed for both vector and parallel processing computer systems. Simulation results have been obtained using a dynamic subgrid-scale model for a channel heated and cooled at temperature ratios as high as 3. Results were also obtained for a channel with uniform wall heat flux heating and cooling with wall to bulk temperature ratios as high as 1.5 for heating and 0.56 for cooling. Density rms fluctuations as high as 9 % have been observed for very low Mach number flows with heat transfer. Mean and rms velocity and temperature data were observed to collapse toward incompressible results when plotted in semi-local coordinates. Preliminary results have also been obtained for flow in a rib-roughened channel. The large eddy simulation algorithms were extended to include the use of unstructured and zonal embedded grids. Particularly, the use of zonal embedded grids show much promise for extending the Reynolds number range for which large eddy simulation can be employed with existing computers.

19980602 089

14. SUBJECT TERMS
Large eddy simulation, turbulent flow, heat transfer

15. NUMBER OF PAGES
i-iii, 1-30, 33 total

16. PRICE CODE

17. SECURITY CLASSIFICATION OF REPORT	18. SECURITY CLASSIFICATION OF THIS PAGE	19. SECURITY CLASSIFICATION OF ABSTRACT	20. LIMITATION OF ABSTRACT
Unclassified	Unclassified	Unclassified	

IOWA STATE UNIVERSITY
OF SCIENCE AND TECHNOLOGY

LARGE EDDY AND UNSTRUCTURED GRID METHODS FOR HEAT TRANSFER APPLICATIONS IN PROPULSION SYSTEMS

Richard H. Pletcher
Department of Mechanical Engineering
and Computational Fluid Dynamics Center
Iowa State University

College of Engineering

Final Technical Report
AFOSR Grant F49620-94-1-0168

Report ISU-ERI-Ames-98405

LARGE EDDY AND UNSTRUCTURED GRID METHODS FOR HEAT TRANSFER APPLICATIONS IN PROPULSION SYSTEMS

Richard H. Pletcher
Department of Mechanical Engineering
and Computational Fluid Dynamics Center
Iowa State University
Ames, Iowa 50011

May 20, 1998

College of Engineering
Iowa State University

TABLE OF CONTENTS

ABSTRACT.....ii

1.0 INTRODUCTION..... 1

2.0 SUMMARY OF RESULTS..... 4

2.1 Overview..... 4

2.2 Numerical Strategy..... 5

2.3 Observations on Discretization Methods..... 6

2.4 Incompressible Flow Results.....11

2.5 Results for Flows with Variable Property Heat Transfer.....14

2.6 Use of Unstructured and Zonal Embedded Grids.....20

3.0 PUBLICATIONS.....26

4.0 PERSONNEL.....28

5.0 REFERENCES.....28

1.0 INTRODUCTION

This report summarizes the research accomplishments achieved under Grant AFOSR F49620-94-1-0168, "Large Eddy and Unstructured Grid Methods for Heat Transfer Applications in Propulsion Systems." The objective of the research was to address some major technological needs that were and still are limiting progress in the development of improved design and predicting capability for modern high performance propulsion systems. The most urgent of these is the need for better methods for predicting the thermal features of turbulent flows that are technologically important. Examples of such flows occur in turbine and combustor components of gas turbine engines. Existing methods were considered inadequate for the accurate prediction of turbulent or transitional flow in configurations of practical interest.

Considering the recent and planned advances in computer hardware, it was believed that the time was right for increased research in direct (DNS) and large eddy simulations (LES), since more and more flows of practical interest were coming within reach of current and planned computers. Extrapolating computer hardware advances into the future, it appears only a matter of time before LES becomes a viable alternative for computing many turbulent flows. It was believed to be important to bring this emerging technology to bear on urgent problems in aeropropulsion systems. The main goal of the research, then, was to expand LES methodology to a broader class of flows with heat transfer to ultimately contribute to the solution of some of the urgent problems that are limiting performance of aeropropulsion systems.

To obtain flow information computationally, one has three possible ways to proceed. Most common in dealing with applied problems are the approaches based on the Reynolds-averaged Navier-Stokes (RANS) equations. Here turbulence modeling plays a major role and results are uncertain or unsatisfactory for many complex flows. It is widely accepted that improvements are essential. The second alternative is direct numerical simulation (DNS). It is well established now that the three-dimensional Navier-Stokes equations along with appropriate forms of the continuity and energy equations govern turbulent flow, but limited computer resources prohibit the resolution of flows characteristic of most applications by DNS. This situation is destined to change eventually. As computer hardware and algorithms improve, the frontier will be continuously pushed back, allowing flows of increasing practical interest to be computed by direct numerical simulations (DNS). The third alternative is LES, in which modeling is required only for the smallest and most universal scales. This is another approach to simulating turbulence that will benefit increasingly with improvements in computer hardware. In fact, it is believed that the time is right for increased research in this area as more and more practical flow conditions come within reach of current and planned computers. The motivation here, in addition to responding to a need for basic understanding of turbulent flows, is the desire to move the LES capability toward geometries and conditions more in line with those occurring in critical application areas.

Applying DNS and LES to more and more realistic configurations involves more than simply waiting for the computing power to become available and then applying a well-established algorithm. Most of the configurations addressed by researchers to date have allowed the use of periodic boundary conditions at inflow and outflow. Such

conditions free the researcher from the task of specifying specific detailed conditions at both inflow and outflow. Effective and efficient ways of dealing with more general inflow and outflow conditions for DNS and LES simulations are generally not known or have likely not been optimized to make the best use of computational resources. Modeling the subgrid-scale (SGS) transport in LES is another issue that needs further development and understanding as more and more complex flows are addressed. Because most of the flows computed by LES to date have been geometrically simple and at low Reynolds numbers, the limitations of existing subgrid-scale models have not been severely tested.

Several facets of LES have been explored under this research program. The results of interest to the technical community can be listed in the following categories:

- Observations and developments on algorithms for LES.
- New results for incompressible flow in a square duct.
- Advances in the use of unstructured and zonal embedded grids.
- New results for channel flows with heat transfer and significant property variations.
- Some innovations on modeling inflow and outflow conditions for LES.

The next section will summarize the results from this research program citing publications where additional details can be found. Copies of dissertations can be obtained from UMI Dissertation Services, Ann Arbor, Michigan. Copies of computer codes can be obtained from Richard Pletcher, Department of Mechanical Engineering, Iowa State University.

2.0 SUMMARY OF RESULTS

2.1 Overview

Major results and innovations:

- A finite volume solution scheme for the compressible Navier-Stokes equations has been developed for large eddy simulation of turbulent flow using Mach number preconditioning to enable efficient solutions of variable property gas flows at low Mach numbers.
- Two promising procedures have been found to eliminate even-odd decoupling of solutions that often occur with the use of colocated grids and central difference numerical schemes. Grid level decoupling (wiggles) was eliminated without deterioration of the accuracy of the turbulence statistics.
- A large eddy simulation of a channel flow with one wall heated and the opposing wall cooled at a temperature ratio of 3 has revealed several interesting features of variable property flows including confirmation of density rms percentage fluctuations of 9% for a flow at M = 0.01.
- For the first time, an LES of channel flow with uniform heat flux and significant property variations for both heating and cooling has been obtained allowing comparisons with experimentally-based correlations in the literature and a determination of structural changes induced by strong property variations.
- Uniform heat flux studies revealed that distributions of mean velocities, temperature, and rms fluctuations of velocities and temperature were strongly influenced by property variations but could be nearly collapsed to constant

property distributions through the use of semi-local coordinates as explained below.

- Work has been initiated toward the use of unstructured grids in LES and the performance of compressible LES formulations on regular and unstructured grids using both a dynamic subgrid-scale model and the Smagorinsky model have been compared for the decay of isotropic turbulence. Most recently, the use of hexahedral control volumes in zonal embedded manner has shown much promise as a means of economically achieving simulations at high Reynolds numbers. The scheme allows for small volumes near solid boundaries but permits coarsening in all three directions. It is possible to obtain good accuracy with a relatively small number of cells. It is believed that a major advance in the simulation of high Reynolds number flows is in progress.

2.2 Numerical Strategy

The numerical formulation used in the research was based on a finite volume discretization of the Favre-filtered compressible Navier-Stokes equations. The approach is thought to be somewhat novel in three respects. First, there have been only a few studies reported in the literature to date in which a fully coupled, compressible formulation has been used for either DNS or LES. Second, an all-speed strategy is being followed in the numerical simulations which permits the same general methodology to be applied to fully incompressible flows, compressible flows at very low Mach numbers where effects of property variations need to be accounted for, and at transonic and supersonic speeds. Basically, this flexibility is achieved by employing a coupled, compressible formulation with low Mach number preconditioning [1]. With

preconditioning, the numerical stiffness and slow convergence associated with traditional compressible formulations are avoided and, in fact, the convergence rate becomes virtually independent of Mach number in the low speed regime. However, for purely incompressible simulations, the scheme can be further streamlined by specializing it to a pseudo-compressibility formulation. This avoids the necessity of solving the energy equation for those flows that are essentially isothermal. To this investigator's knowledge, no other DNS or LES scheme has this generality. Third, effects of heat transfer were considered. Although some heat transfer results have appeared in the literature, available results are very limited, especially for separated flows, and usually do not take into account effects of variations in fluid properties.

Within this framework, several schemes that differ in detail have been employed. The variations arose due to searches for increased accuracy, economy, and the ability to accommodate geometric complexity. This has led to evaluations of upwind and central schemes in the search for accuracy. Variations suitable for vector machines such as the Cray C90 and parallel systems such as the IBM SP2 and SGI Origin 2000 were considered in the search for economy. Use of unstructured and zonal embedded grids was motivated by interest in computational economy and the long-term need to deal with complex geometry.

Further information on the numerical formulations employed and lessons learned will be given in the following section.

2.3 Observations on Discretization Methods

The first lesson learned was that performance on traditional laminar flows in not a reliable indication of performance to be expected for use in LES. One reason for this is

that achieving accurate LES results requires that very many length and time scales be accurately resolved whereas most laminar flow problems are characterized by relatively few critical scales. This observation was pointed out in dissertation research completed by Wang [2,3], where it was noted that calculations performed on both staggered and colocated grids gave identical results for several laminar test cases but the staggered grid results were better and the scheme more robust when applied for LES. Further, an upwind scheme employing third-order upwinding for advective terms and fourth-order central viscous discretization gave very accurate results in laminar test cases but often failed to out-performed a second-order central representation for LES applications. The upwind scheme was found to be the most robust scheme, however. Central difference schemes, especially on colocated grids, were observed to fail due to apparent instability for some simulations early in the research program.

For completeness, it should be mentioned that more recent studies [4] have demonstrated that some of the stability problems encountered by Wang was likely due to choices made in interpolating fluxes to cell faces. Wang [2,3] interpolated the fluxes themselves, but Chidambaram [4] was able to show that construction of cell face fluxes from the interpolated primitive variables was more robust than interpolating the fluxes. When the central difference schemes of Wang [2,3] were modified to compute the fluxes from interpolated primitive variables, robustness appeared to be restored and a failure due to stability on regular grids has not been observed to date. Chidambaram [4] discusses the probable cause for this behavior.

From time to time when simulating low-speed flows on a colocated grid, decoupling of the solution can be observed giving rise to grid-frequency oscillations or "wiggles" in

the solution, particularly the pressure. This is a very well known effect encountered by many investigators. The cause is associated with the physical requirement to represent the pressure gradient with a central difference at low speeds. This effect can be eliminated with the use of a staggered grid; however, colocated grids are much more convenient to deal with, especially when computing flows in complex geometries or when using unstructured grids. In our research the wiggles were not always a problem, but tended to occur when dealing with a complex geometry like the ribbed channel or when simulating flows at high Reynolds numbers. Use of traditional artificial dissipation to remove such oscillations typically causes significant deterioration in the accuracy of LES calculations.

Two promising solutions to the decoupling were developed in the research. Chidambaram [4] developed a momentum interpolation correction procedure that effectively coupled velocities and pressure. A similar procedure has been developed by Rhie and Chow [5] and others for colocated schemes that solved the equations in an uncoupled (pressure-correction) manner. However, Chidambaram [4] appears to be the first to derive and employ an appropriate interpolation scheme for the compressible Navier-Stokes equations solved as a coupled system.

An alternative promising procedure that is being evaluated at present employs a sixth order compact filter [6] that appears to minimize or eliminate grid-frequency oscillations without damping the solution otherwise. An example of grid-frequency oscillations can be seen in the contours of mean streamwise velocity in a rib-roughened channel shown in Fig. 1. Ribbed channels are somewhat characteristic of the internal cooling passages of gas turbine engine blades. The LES solution employed a dynamic subgrid-scale model

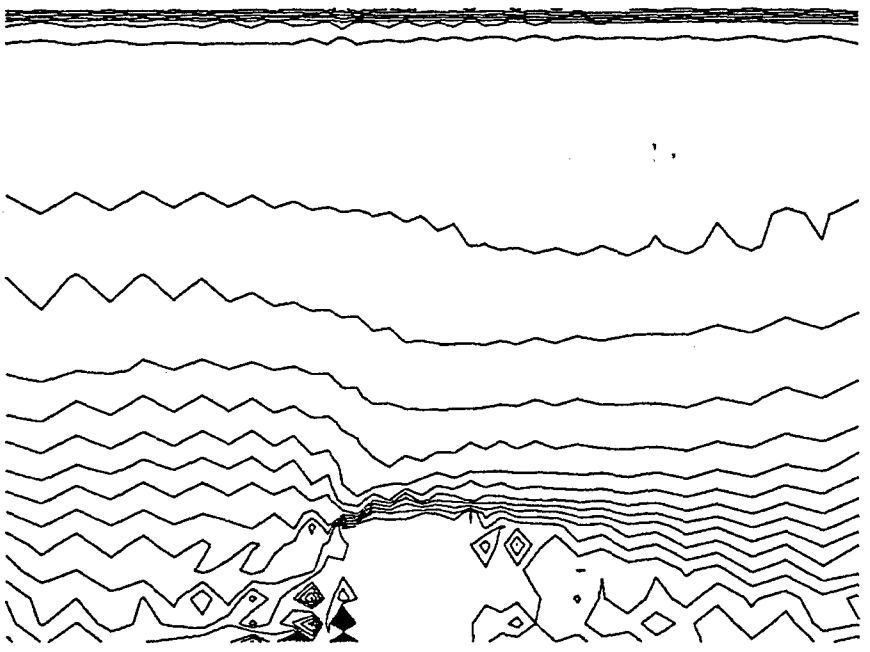

Figure 1. Contours of streamwise component of mean velocity for flow in a rib-roughened channel, unfiltered solution.

on a grid composed on $40 \times 32 \times 24$ control volumes. The simulation was at a Reynolds number of 20,000 based on the hydraulic diameter. The ratio of the rib height to the channel height was 0.2 and the rib streamwise spacing was 7.2 channel heights. Figure 2 shows the velocity contours when the sixth order filter was employed. Figure 3 compares the present LES results (with filtering) for the mean streamwise velocity midway between ribs with experimental data [7,8] and the LES simulations of Ciofalo and Collins [9]. The agreement with experimental data is encouraging. Notice that a small region of recirculation is present at this location, 3.6 rib-heights downstream. Figure 4 compares the rms streamwise velocity distribution at the same location. Again, the agreement with measurements is encouraging. Although not shown here, the effect of filtering on the mean velocities is almost indiscernible on plots. Small changes can be seen in rms

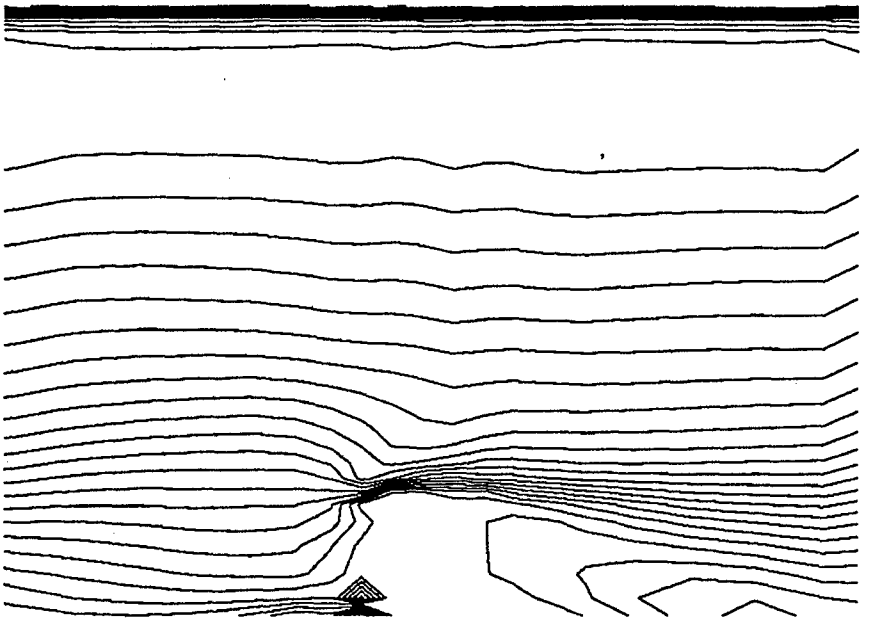

Figure 2. Contours of streamwise component of mean velocity for flow in a rib-roughened channel, filtered solution.

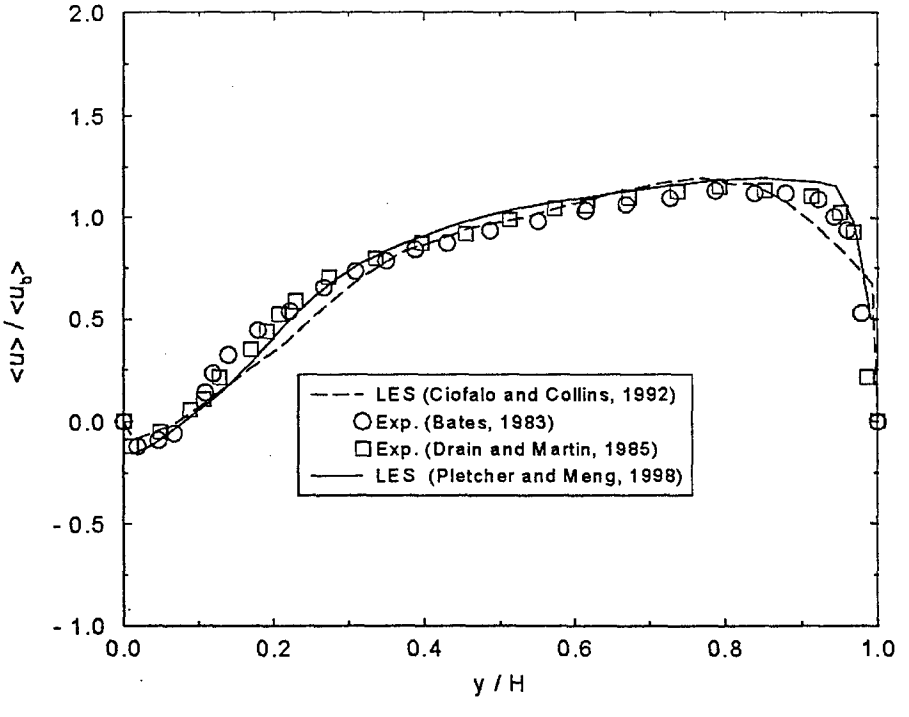

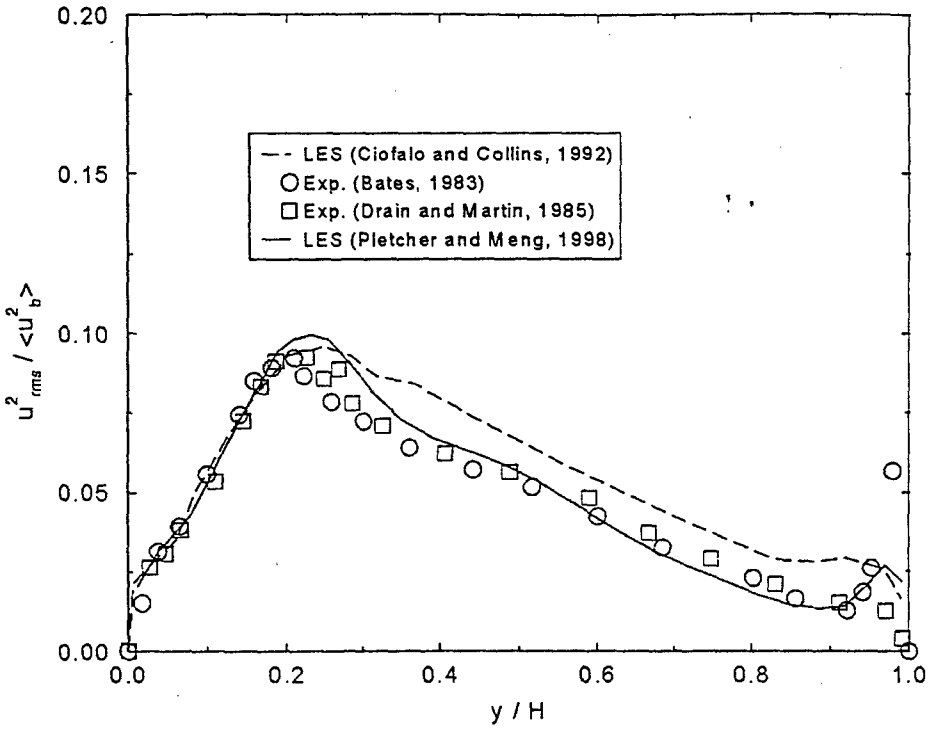

Figure 4. RMS streamwise velocity fluctuations midway between ribs normalized by bulk velocity, filtered solution.

quantities, but the filtered solution tends to agree best with the experimental data. This is work in progress, and full results have not yet been published.

2.4 Incompressible Flow Results

Although the main thrust of the research involved an "all-speed" compressible formulation, some aspects of the approach were evaluated first through computations with an incompressible formulation in order to conserve computer resources. Also, it was then possible to too take advantage of the greater abundance of experimental and computational results available for comparison in the incompressible regime. Furthermore, before attempting LES or DNS simulations with any algorithm, a number of traditional two and three-dimensional flows were computed including the three-

dimensional driven cavity and the growth of a small disturbance in a two-dimensional channel. Such results are described in the dissertations by Wang [3] and Dailey [10]. The evolution of a small disturbance was considered particularly useful in screening candidate discretization schemes for temporal and spatial accuracy.

The incompressible planar channel flow at a bulk Reynolds number of about 5500 was the primary flow chosen to demonstrate the capability of the schemes developed to perform large eddy simulations of turbulent flow. The merits of the schemes and subgrid-scale models were gauged by comparisons with the fine grid DNS results of Kim et al. [11] which used four-million grid points and the experimental work of Niederschulte et al. [12]. Eight different combinations of the three different spatial algorithms (i.e., 2CD, 4CD and UPWIND), combinations of the regular/staggered grid arrangements, and two different SGS models were evaluated. Effects of grid refinement were included in the study. Extensive comparisons between the calculated results obtained with the various discretizations, grids, and subgrid-scale models can be found in [2,3].

A second configuration simulated with the dynamic model and the incompressible formulation was turbulent flow in a square duct at a Reynolds number of about 9500 based on the bulk velocity and duct width. To the principle investigator' knowledge, this was the first time that the dynamic model had been used for this configuration. For the square duct flow, laboratory experiments have indicated that if the flow is turbulent the contours of mean axial velocity bulge toward the corner due to a secondary flow pattern in the cross-section. This phenomenon is not observed in a circular duct flow or in the laminar flow of a non-circular duct. This is the well-known "secondary flow of the

second kind." The secondary flow is caused by the highly anisotropic and inhomogeneous nature of the turbulence stresses near the intersection of the walls.

Numerical calculations of non-circular duct flows using the Reynolds-averaged equations were first performed in the early 1970s. However, due to the highly anisotropic nature of the turbulence near the corner, a turbulence closure model based on the flow isotropy assumption, e.g., the $k-\varepsilon$ (two-equation) model, fails to resolve the secondary flow (unless, special provisions like using a nonlinear form of the two-equation model [13] was employed). A second-order Reynolds stress model can recognize the flow anisotropy. Nevertheless, the empiricism used in the modeling of the various correlation terms in the Reynolds stress transport equation has restricted the generality of the model. In this respect, DNS/LES may provide an alternative tool to study the more complicated near-wall turbulence induced by the secondary flow.

The simulation was carried out on a $65\times65\times65$ grid with a computation domain of $2\pi D\times D\times D$, where D is the duct width. Since there was only one homogeneous direction, sample points had to come mainly from the time step solution; this extended the number of time steps needed to collect enough samples to make the statistics stationary.

Figure 5 shows the cross-stream secondary velocity vectors in the lower left quadrant. Obviously, the secondary flow exhibits a high degree of symmetry with respect to the corner angle bisector (although more sample points are probably needed to achieve perfect symmetry). The computed secondary flow pattern agrees with experimental observations with the flow being toward the corner along the corner angle bisector and away from the corner along the walls. The maximum amplitude of this

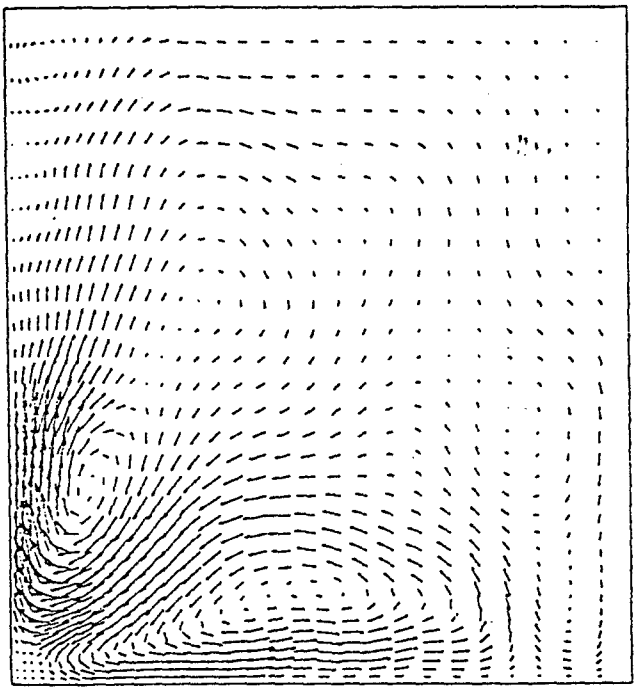

Figure 5. Secondary flow velocity vectors in the lower-left quadrant, square duct, Re_c = 11,500, dynamic model.

secondary velocity was 1.5% of the bulk flow. Results were compared with data available in the literature. Additional comparisons on this case can be found in [2,3].

Comparisons were also made with incompressible results to validate the several discretizations and models employed by using a compressible formulation at very low Mach numbers. Flows simulated in this manner included the decay of isotropic turbulence as well as the channel flow. These results have been reported in [4,10, 14-16].

2.5 Results for Flows with Variable Property Heat Transfer

Two heating/cooling arrangements have been studied to date in this research. The first was a channel heated on one side and cooled at the same rate on the opposite side. Temperature ratios of 1.02 and 3.0 were employed. The simulations were carried out for air at a nominal Mach number of 0.01 and a Reynolds number based on centerline

properties and channel half width of about 3200 and a Prandtl number of 0.71. An implicit compressible upwind scheme that was fourth order accurate in the viscous terms and third-order accurate in the advective terms was used on a $65 \times 65 \times 65$ grid that spanned a $2\pi\delta \times 2\delta \times \pi\delta$ domain where δ is the channel half width. The grid in the wall-normal direction was stretched resulting in the point closest to the wall being located at $y^+ = 0.92$. As can be seen in Fig. 6, the van Driest transformation did not collapse the simulation data onto the incompressible law of the wall for the case with the highest heat transfer rate (HIGH). The results labeled LOW were obtained using a temperature ratio of 1.02.

Although the Mach number was in the nominally incompressible range, density rms percentage fluctuations were about 9% near the cold wall (Fig. 7). This is almost as large as the density rms fluctuations observed by Coleman et al. [17] in their DNS results for channel flow at a Mach number of 3.0. Although this was initially surprising, it becomes plausible when viewed in the following way. It is reasonable that the overall temperature difference in the flow be the scaling factor to determine the order of magnitude of the temperature fluctuations. Indeed, when the T_{rms} distributions for the two cases are nondimensionalized by half the difference in wall temperatures (curve labeled "original"), the distributions for the two cases do, in fact, agree in order of magnitude (but not detail) as can be seen in Fig. 8. That being the case, then it follows that on a local percentage basis, T_{rms} is expected to achieve a larger value near the cold side than near the hot side. Note, however, that on an absolute basis, the T_{rms} peaks near the hot wall would be about 7% larger than near the cold wall. Similarly, the velocity rms peaks were observed to be somewhat larger near the hot wall than near the cold wall. Somewhat unexpectedly, the

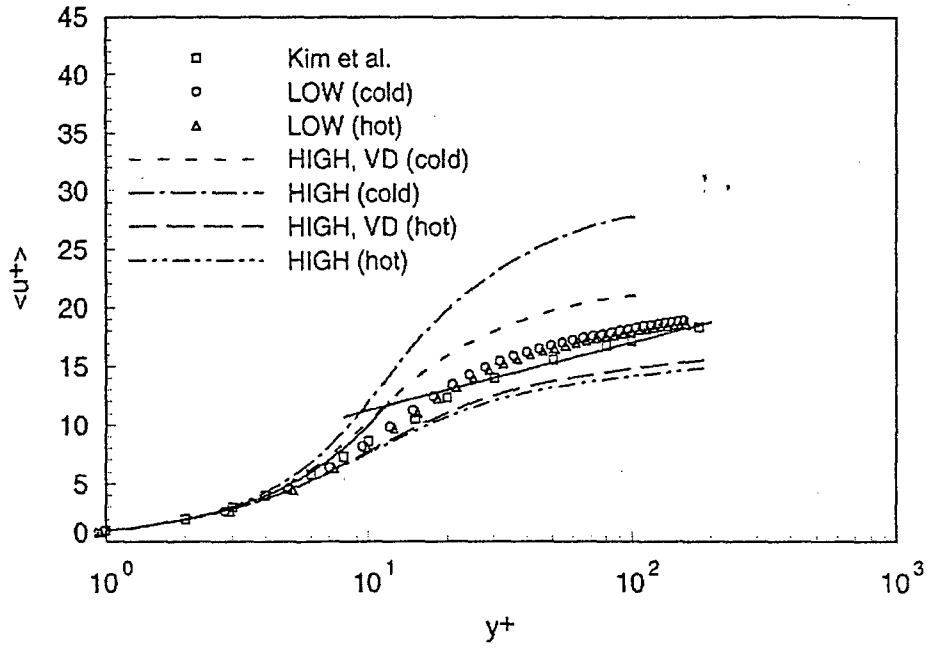

Figure 6. Mean velocity profile in wall coordinates for channel showing effects of high heat transfer rates.

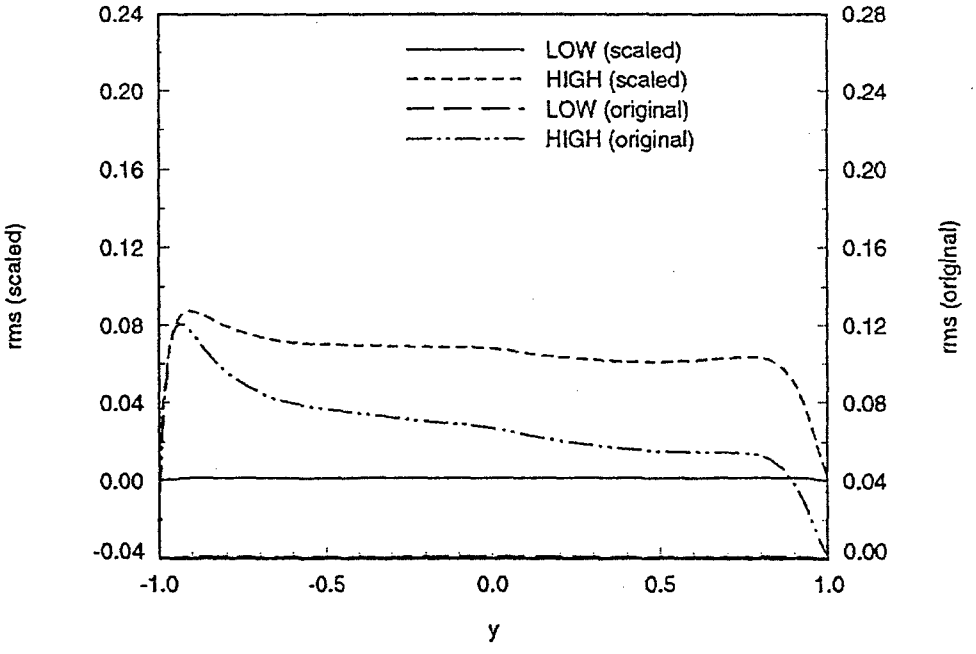

Figure 7. Distribution of ρ_{rms} across channel; scaled: $\rho_{rms}/\langle\rho\rangle$; original: ρ_{rms}/ρ_{ref}.

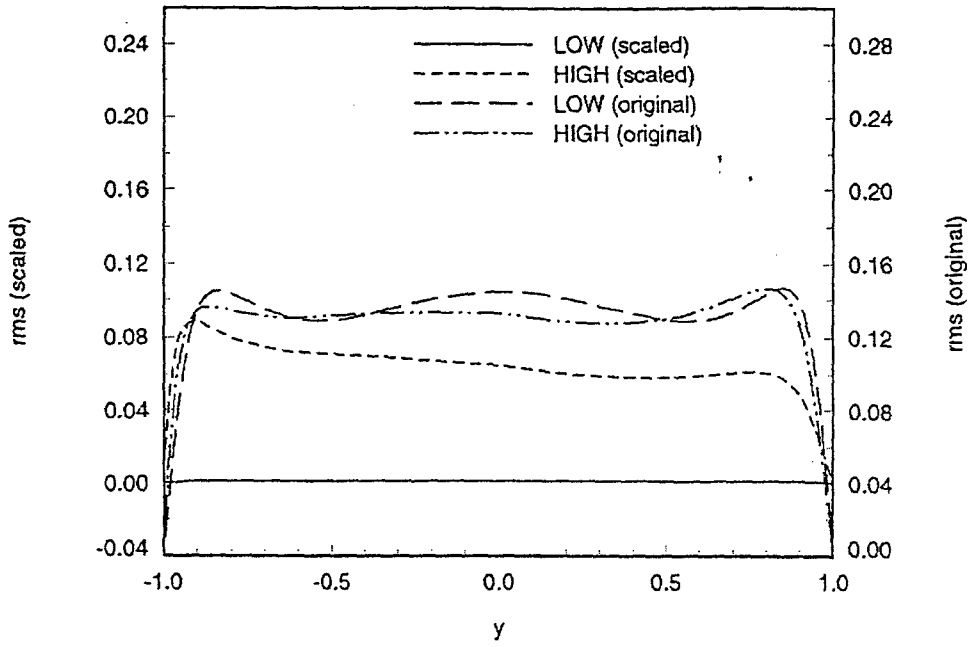

Figure 8. Distribution of T_{rms} across channel; scaled: $T_{rms}/\langle T\rangle$; original: $2T_{rms}/(T_{hot}-T_{cold})$.

wall shear stress was observed to be about 17% greater on the hot wall than on the cold wall. Other relevant results such as the shear stress and heat flux budgets, distributions of $-\langle T'v'\rangle$, skewness, flatness, and correlation coefficients can be found in [3,18].

As for the density, this study as well as others at higher Mach numbers indicate that the mean flow is nearly isobaric. If it is assumed to be so, and the pressure percentage fluctuations are assumed to be small, then one can deduce that $\rho_{rms}/\langle\rho\rangle \approx T_{rms}/\langle T\rangle$. By computing the density rms values from this relationship, one obtains agreement within 2% of the results shown in Fig. 7. Coleman et al. [17] observed similar trends for $\rho_{rms}/\langle\rho\rangle$ and $T_{rms}/\langle T\rangle$ for their M = 3 results, i.e., an indication of nearly isobaric behavior.

Not all of the above observations were expected, so a follow-on series of large eddy simulations were conducted in order to shed more light on the effects of property variations on turbulent channel flow. For this purpose, channel flow with a uniform heat

flux was utilized since such a configuration is much more common in applications than the hot-cold isothermal wall case discussed above. The uniform heat flux flow undergoes bulk heating or cooling so that periodic boundary conditions in the streamwise direction cannot be used in a strict sense. In the present simulations, periodicity in the streamwise density-velocity product was assumed. The temperature and pressure were assumed to be step-periodic with the temperature step being computed from an energy balance utilizing the imposed wall heat flux and a mean pressure gradient being established of such a magnitude so as to maintain the desired mean mass flow rate. The results to be shown here were obtained on a grid that used $48 \times 64 \times 48$ control volumes. The value of y^+ at the near-wall control volume was approximately unity. The Smagorinsky subgrid-scale model was used (C_s = 0.08) with van Driest-type damping. Further details on the numerical formulation can be found in [10,15].

Three cases have been computed, all for an inlet Reynolds number of approximately 11,000 based on bulk properties and the hydraulic diameter and a Mach number of 0.001 based on inlet bulk properties. These were a low heating ($T_w/T_b = 1.025$), a high heating ($T_w/T_b = 1.485$), and a high cooling ($T_w/T_b = 0.564$) case. The low heating was selected in order to compare with the passive scalar DNS results of Kasagi et al. [19]. Most experimental studies of heat transfer in turbulent internal flows have been carried out in tubes rather than channels. Kakac [20] points out that noncircular channel friction factor and Nusselt number results are expected to be within 10-15% of circular tube values with the parallel plate channel results being 7-11% high. Indeed, that trend was confirmed by the present simulations. The Nusselt numbers based on bulk properties obtained from the simulations were 34.52, 30.77 and 33.99 for the low heating, high heating, and high

cooling cases, respectively. The corresponding skin-friction coefficients were 0.007683, 0.007822, and 0.007787. Comparisons have been made with several correlations of experimental data, and the correlation values of skin-friction coefficient and Nusselt number tended to be within $\pm 8\%, 20\%$, and 13% for the low heating, high heating, and high cooling cases, respectively. Generally, the Nusselt numbers based on bulk properties from the simulations did not show as much sensitivity to wall to bulk temperature ratios as indicated by the correlations. Most of the experimental data were obtained at Reynolds numbers higher than used in the simulations; however, several correlations were claimed to be valid for the Reynolds number of the present simulations. Although experimental data are available for global engineering parameters under high heat transfer conditions, relatively little information exists on detailed velocity and temperature profiles and the statistical features of such flows.

The maximum density rms percentage fluctuations were again observed to be in the 9% range for this "incompressible," M = 0.001 flow. The near-wall rms values were greater for the high cooling case than for the high-heating case, which is consistent with the observations reported above for the hot-cold isothermal wall channel flow. The distribution of the temperature rms percentage fluctuations (not shown) was nearly identical to that of the density, a consequence of the flow being essentially locally isobaric. One of the most relevant findings of this study was that many of the results from the simulations for both heating and cooling tend to collapse toward the same distribution when plotted in semi-local coordinates. Such a collapse had been noted by others for high speed flow, but this is the first report of a similar trend for nominally "incompressible" flow. The semi-local coordinates are obtained by using local properties

(density and viscosity) when computing the friction velocity (wall shear stress divided by local density) and y^+. An asterisk will be used to denote the semi-local coordinates rather than $^+$.

Figure 9 shows the mean velocity profile in conventional wall coordinates for the three heat flux cases. For reference, the constant property DNS data of Kim et al. [11] and the experimental data of Niederschulte [12] are shown on the figure. A clear dependence on the wall to bulk temperature ratio is evident. When the data are plotted in semi-local coordinates, Fig. 10, the spread in the curves is greatly reduced. A similar effect was observed for the mean temperature profile and again the data were significantly compressed by use of semi-local coordinates. The remarkable thing is that this near similarity extends to distributions of fluctuating quantities, also. Figure 11 shows the distribution of rms velocity components plotted in traditional wall coordinates, and Fig. 12 shows the same data plotted in semi-local coordinates. Notice how the transformation shifts the location of the maximums and tends to collapse the three rather different curves into a single distribution. Clearly, the collapse, while significant, isn't perfect. Further results from the constant heat flux simulations are described in [10,21].

2.6 Use of Unstructured and Zonal Embedded Grids

Research on the use of both unstructured and zonal embedded grids has been completed as part of this project. Unstructured grids allow the flexibility of placing computational cells within the problem domain in an arbitrary manner. Typically, cells composed of tetrahedra or hexahedra are used. The zonal embedded grids considered here employed zones of hexahedral cells. Each zone was treated in a structured manner

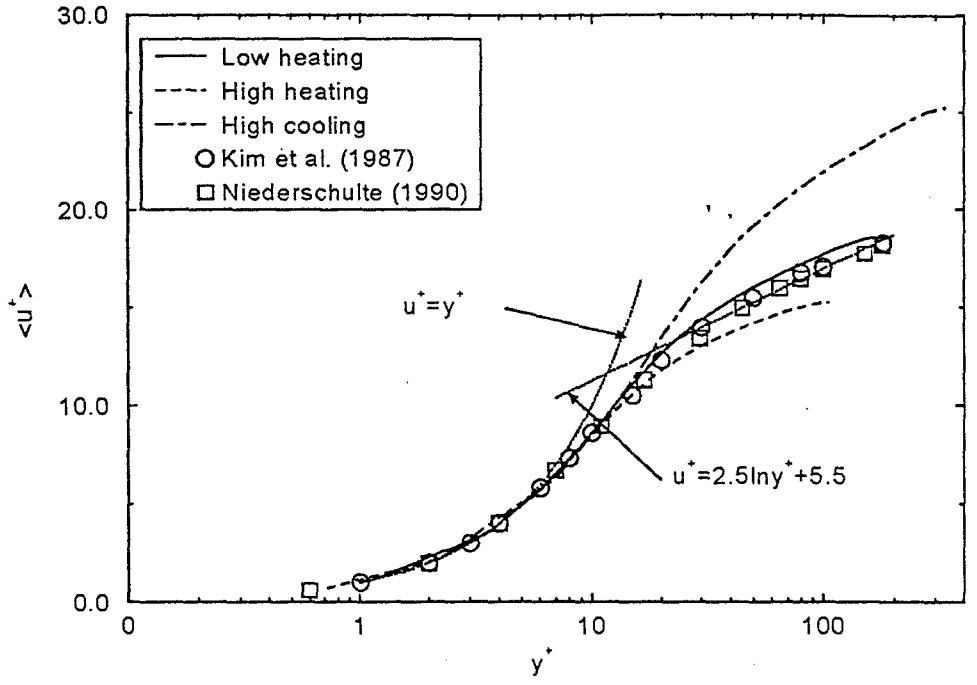

Figure 9. Mean streamwise velocity in wall coordinates; channel flow with uniform heat flux heating and cooling.

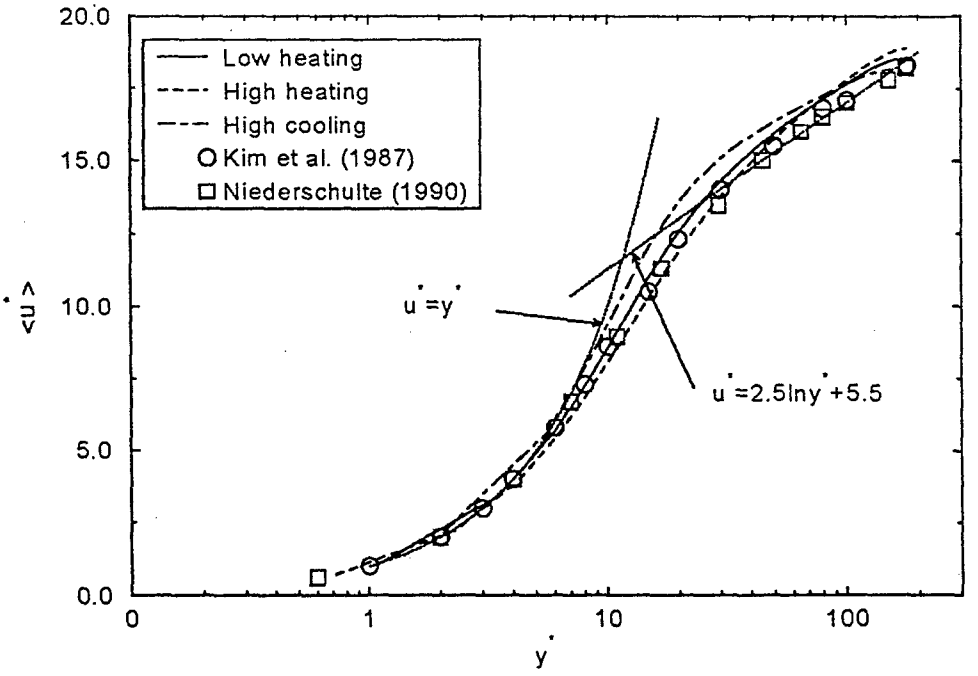

Figure 10. Mean streamwise velocity in semi-local coordinates; channel flow with uniform heat flux heating and cooling.

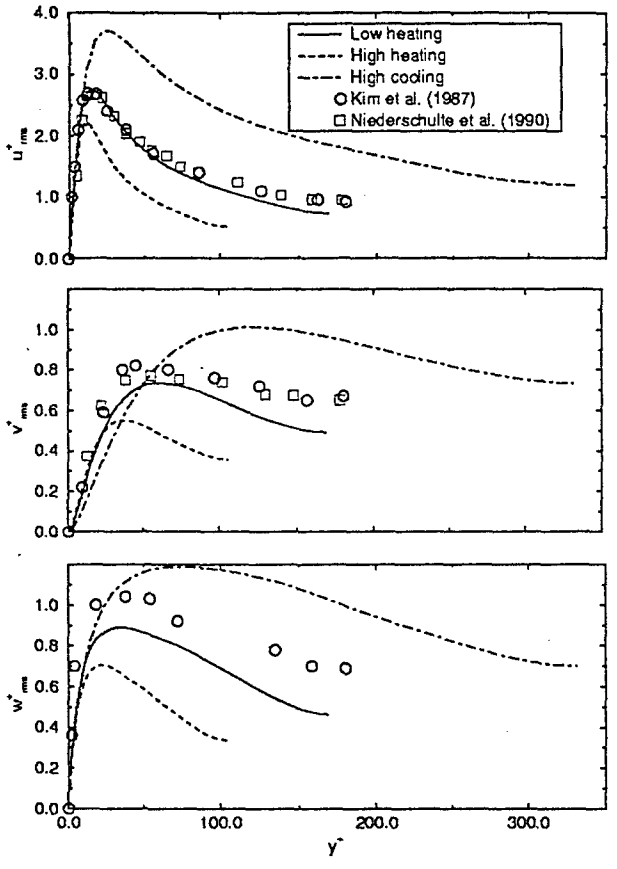

Figure 11. Velocity fluctuations in wall coordinates with uniform heat flux heating and cooling.

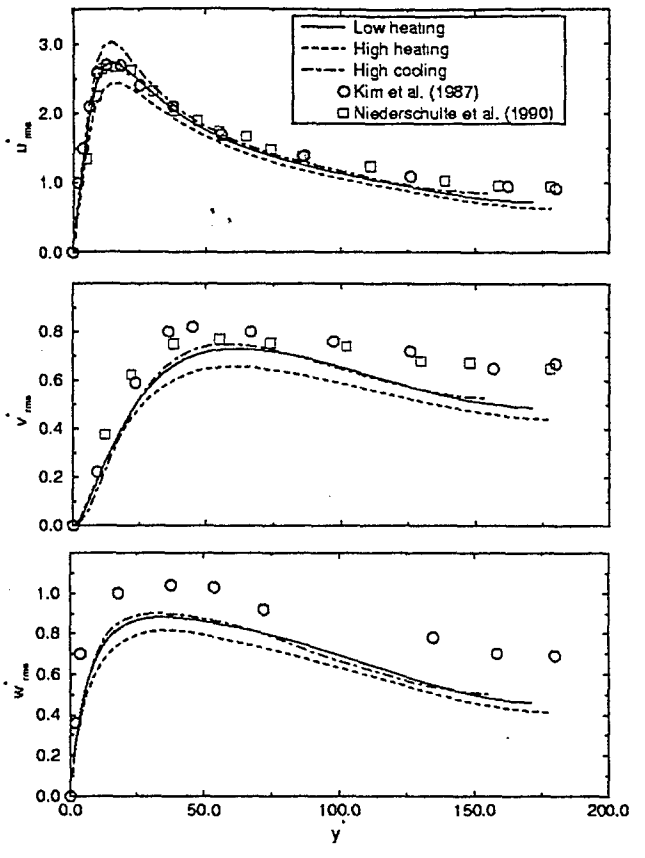

Figure 12. Velocity fluctuations in semi-local coordinates with uniform heat flux heating and cooling.

and interpolation was used at zone interfaces. Fine grid zones can be placed in regions where greater spatial resolution is required.

The use of such grids is an attractive alternative for dealing with geometrically complex flows. As computing hardware continues to improve, DNS and LES will be applied to flows of increasing complexity. Thus, it was considered appropriate to begin to understand the advantages and limitations associated with the use of unstructured and zonal embedded grids for LES and DNS. Also, the use of such grids provides the ability to cluster computational cells near all solid boundaries while permitting a more sparse distribution in the interior of the domain. Then, if algorithm accuracy can be maintained on the unstructured and embedded grids, less computational effort will be required to

perform a simulation of given accuracy than would be required on a more traditional structured grid.

The unstructured grid scheme has been applied to the LES of isotropic decaying turbulence using a grid composed of tetrahedrons with encouraging results. These results were reported in [14]. More recent unstructured grid results will be reported in [16]. For flows along solid boundaries, the use of zonal embedded hexahedral control volumes has shown much promise as a means of economically achieving simulations at high Reynolds numbers. The scheme allows for small volumes near solid boundaries, but coarsening in all three directions is possible, leading to good accuracy with a relatively small number of cells. It is believed that a major advance in the simulation of high Reynolds number flows is in progress. The only other known LES application of zonal embedded grids was reported by Kravchenko et al. [22]. They solved the incompressible equations using a spectral method in two directions and a Galerkin method with B-spline basis functions in the third direction. The present form of their method can only be applied to a very limited class of problems compared to the present finite volume method for solving the fully compressible equations.

Sample LES simulations have been carried out for channel flow using a zonal embedded grid. A projection of such a grid on the x-y plane is shown in Fig. 13. The grid shown was used for a flow at an approximate Reynolds number of 3,500. There were 5 zones across the channel, symmetrically positioned about the channel centerline containing a total of 128,736 cells. The resolution of the near wall region is $64 \times 9 \times 64$. Domain decomposition can be easily used to achieve good load balance on parallel processing machines such as the Origin 2000. A simple structured grid with the

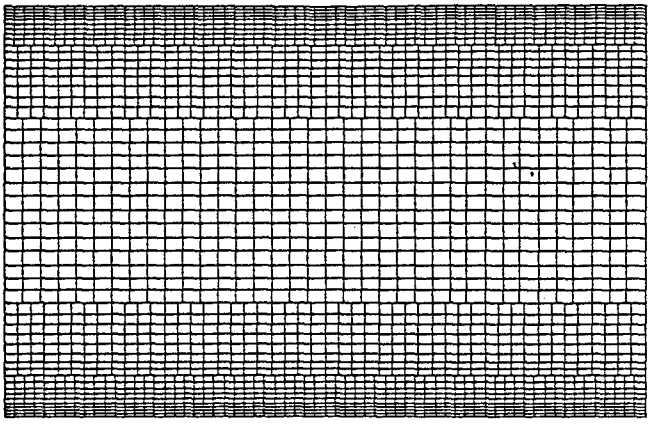

Figure 13 Two-dimensional projection of a zonal embedded grid.

equivalent near wall resolution would require roughly twice as many grid points (64^3) as the zonal embedded grid. This represents considerable savings in CPU cost (an estimated factor of 4-6).

One of the challenges with zonal grids is to provide smooth and conservative transitions across zonal boundaries. Figure 14 shows rms fluctuation results for the Re = 3,500 case mentioned above. Zonal boundaries are marked on the figure. The solutions appear to be smooth across the boundaries confirming the merits of the interpolation scheme used at the zonal interfaces. Simulation results obtained with both the Smagorinsky and dynamic subgrid-scale models are shown along with the fine grid DNS results of Kim et al. [11]. Further results using the zonal embedded grid are shown in Figs. 15 and 16 for channel flow at the much higher Reynolds number of 21,000 based on the mean streamwise velocity and channel half-height. Results were obtained with both the Smagorinsky and the dynamic subgrid-scale models. Comparisons are made with the experimental data of Wei and Willmarth [23] and the LES results of Piomelli [24] and Najjar and Tafti [25]. The intermmediate grid results were obtained using a near wall

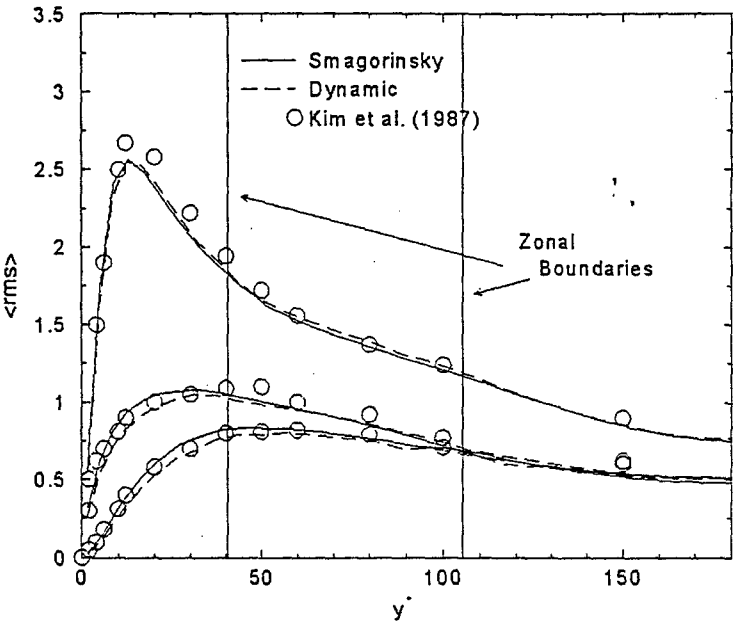

Figure 14. Velocity rms fluctuations (u, v, w components from top to bottom) for Re = 3,500, zonal embedded grids.

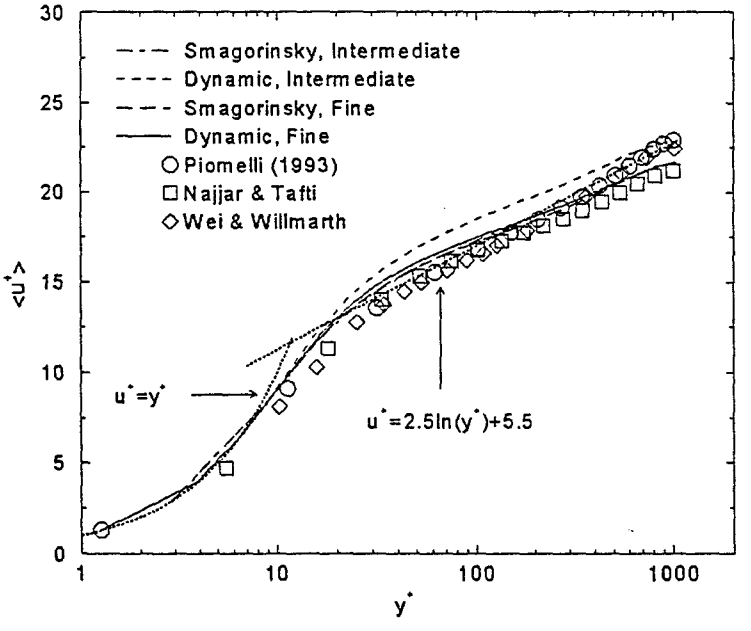

Figure 15. Mean streamwise velocity in wall coordinates, Re = 21,000, zonal embedded grids.

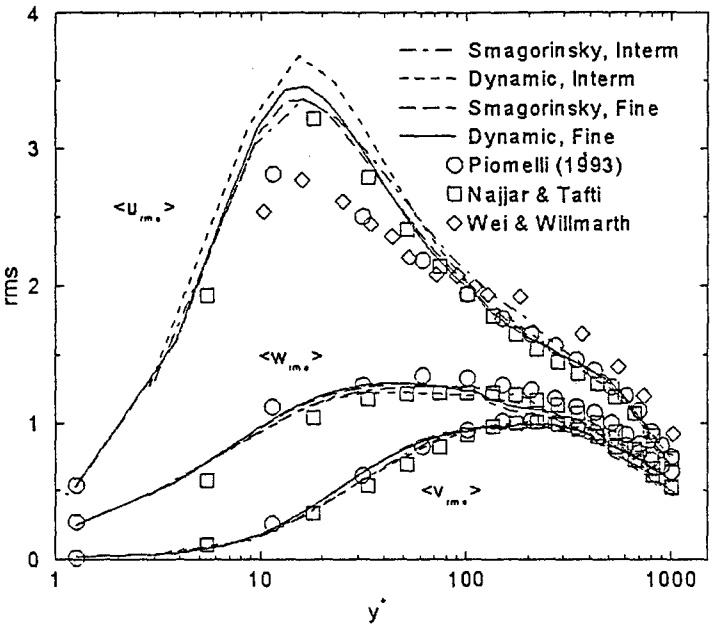

Figure 16. Velocity rms fluctuations for Re = 21,000, zonal embedded grids.

resolution of 70 × 70, a middle zone of 60 × 60, and a core region of 50 × 50. The fine grid employed a near wall resolution of 80 × 80, a middle zone of 64 × 64, and a core region of 50 × 50. Although this work is not yet complete, it appears that the use of zonal embedded grids allows greater accuracy to be achieved for a fixed number of cells than is possible using finite difference methods with traditional grid procedures.

3.0 PUBLICATIONS

Dissertations that describe research that has been supported wholly or in part by this grant include:

Wang, W.-P., 1995. Coupled compressible and incompressible finite volume formulations of the large eddy simulation of turbulent flow with and without heat transfer, Ph.D. dissertation, Iowa State University.

Dailey, L. D., 1997. Large eddy simulation of complex turbulent flows with variable property heat transfer using finite volume methods, Ph.D. dissertation, Iowa State University.

One Masters thesis described work that was partially supported by this grant:

Chidambaram, N., 1998. Colocated-grid finite volume formulation for the large eddy simulation of incompressible and compressible turbulent flows.

Journal articles published or under review that describe research that has been supported wholly or in part by this grant include:

Wang, W.-P. and R. H. Pletcher, 1996. On the large eddy simulation of a turbulent channel flow with significant heat transfer. *Physics of Fluids* 8(12): 3354-3366.

Dailey, L. D. and R. H. Pletcher, 1998. Large eddy simulation of constant heat flux turbulent channel flow with property variations. Submitted to *Physics of Fluids*.

Conference proceedings and preprinted meeting papers that describe research that has been supported wholly or in part by this grant include:

Wang, W.-P., and R. H. Pletcher, 1995. Large eddy simulation of a low Mach number channel flow with property variations. Proceedings of the 10th Turbulent Shear Flow Symposium, pp. 3-73—3-78, Pennsylvania State University.

Wang, W.-P. and R. H. Pletcher, 1995. Evaluation of some coupled algorithms for large eddy simulation of turbulent flow using a dynamic SGS model. AIAA Paper 95-2244.

Dailey, L. D., T. A. Simons, and R. H. Pletcher, 1996. Large eddy simulation of Isotropic decaying turbulence with structured and unstructured grid finite volume methods. FED-Vol. 242, Proceedings of the ASME Fluids Engineering Division, pp. 245-252.

Dailey, L. D., and R. H. Pletcher, 1997. Evaluation of a second-order accurate compressible finite volume formulation for the large eddy simulation of turbulent flows, Proceedings of the First AFOSR International Conference on Direct Numerical Simulation and Large Eddy Simulation.

Dailey, L. D. and Pletcher, R. H., 1998. Large eddy simulation of constant heat flux turbulent channel flow with property variations, AIAA Paper No. 98-0791.

Simons, T. and R. Pletcher, 1998. Large eddy simulation of turbulent flows using unstructured grids. AIAA Paper 98-3314, to be presented at the AIAA/ASME/ASE Joint Propulsion Conference, July, 1998.

4.0 PERSONNEL

Professor R. H. Pletcher served as the Principle Investigator throughout the duration of this grant. Graduate Student Research Assistants that participated in the research include Ravikanth Avancha, Narayanan Chidambaram, Prantik Mazumder, Ning Meng, Todd Simons, and W.-P. (Ben) Wang. In addition, Lyle Dailey assisted significantly in the project although his salary support was obtained from a Department of Defense Fellowship and the General Electric Company.

5.0 REFERENCES

1. Pletcher, R. H., and K.-H. Chen, 1993. On solving the compressible Navier-Stokes equations for unsteady flows at very low Mach numbers. AIAA Paper No. 93-3368-CP presented at the 11th Computational Fluid Dynamics Conference.

2. Wang, W.-P. and R. H. Pletcher, 1995. Evaluation of some coupled algorithms for large eddy simulation of turbulent flow using a dynamic SGS model. AIAA Paper 95-2244.

3. Wang, W.-P., 1995. Coupled compressible and incompressible finite volume formulations of the large eddy simulation of turbulent flow with and without heat transfer. Ph.D. dissertation, Iowa State University.

4. Chidambaram, N., 1998. Colocated-grid finite volume formulation for the large eddy simulation of incompressible and compressible turbulent flows. M.S. thesis, Iowa State University.

5. Rhie, C. M. and W. L. Chow, 1983. Numerical study of the turbulent flow past an airfoil with trailing edge separation. *AIAA Journal*, 21: 1525-1532.

6. Lele, S. K., 1992. Compact finite difference schemes with spectral-like resolution. *Journal of Computational Physics*, 103: 16-42.

7. Bates, C. J., M. L. Yeoman, and N. S. Wilkes, 1983. Non-intrusive measurements and numerical comparison of the axial velocity components in a two-dimensional flow channel for a backward-facing step and a rib-roughened surface. Harwell Report AERE-R 10787, U. K.

8. Drain, L. E. and S. Martin, 1985. Two component velocity measurements of turbulent flow in a ribbed-wall flow channel. Proc. Int. Conf. On Laser Velocimetry--Advances and Applications, Manchester, U. K.

9. Ciofalo, M. and M. W. Collins, 1992. Large-eddy simulation of turbulent flow and heat transfer in plane and rib-roughened channels. *International Journal for Numerical Methods in Fluids* 15: 453-489.

10. Dailey, L. D., 1997, Large eddy simulation of complex turbulent flows with variable property heat transfer using finite volume methods, Ph.D. dissertation, Iowa State University.

11. Kim, J., P. Moin, and R. Moser. 1987. Turbulence statistics in fully developed channel flow at low Reynolds numbers. *J. Fluid Mech.* 177:133-166.

12. Niederschulte, M. A., R. J. Adrian, and T. J. Hanratty, Measurements of Turbulent Flow in a Channel at Low Reynolds Numbers, Experiments in Fluids, 1990, 9: 222-230.

13. Speziale, C. G., 1987. On nonlinear k and k-ε models of turbulence. *Journal of Fluid Mechanics*, 178: 459-475.

14. Dailey, L. D., T. A. Simons, and R. H. Pletcher, 1996. Large eddy simulation of liotropic decaying turbulence with structured and unstructured grid finite volume methods. FED-Vol. 242, Proceedings of the ASME Fluids Engineering Division, pp. 245-252.

15. Dailey, L. D., and R. H. Pletcher, 1997. Evaluation of a second-order accurate compressible finite volume formulation for the large eddy simulation of turbulent flows, Proceedings of the First AFOSR International Conference on Direct Numerical Simulation and Large Eddy Simulation.

16. Simons, T. and R. Pletcher, 1998. Large eddy simulation of turbulent flows using unstructured grids. AIAA Paper 98-3314, to be presented at the AIAA/ASME/ASE Joint Propulsion Conference, July, 1998.

17. Coleman, G. N., J. Kim, and R. D. Moser, 1995. A numerical study of turbulent supersonic isothermal-wall channel flow. *Journal of Fluid Mechanics* 305: 159-184.

18. Wang, W.-P. and R. H. Pletcher, 1996. On the large eddy simulation of a turbulent channel flow with significant heat transfer. *Physics of Fluids* 8(12): 3354-3366.

19. Kasagi, N., Y. Tomita, and A. Kuroda, 1992. Direct numerical simulation of passive scalar field in a turbulent channel flow. *Journal of Heat Transfer*, 114: 598-606.

20. Kakac, S., 1987. The effect of temperature-dependent fluid properties on convective heat transfer. *Handbook of Single-Phase Convective Heat Transfer*, Kakac, S., Shah, R. K., and Aung, W., eds., John Wiley and Sons, New York, pp. 18.1-18.56.

21. Dailey, L. D. and R. H. Pletcher, 1998. Large eddy simulation of constant heat flux turbulent channel flow with property variations, AIAA Paper No. 98-0791.

22. Kravchenko, A. G., P. Moin and R. Moser, 1996. Zonal embedded grids for numerical simulation of wall-bounded turbulent flows. *Journal of Computational Physics*, 127: 412-423.

23. Wei, T., and W. Willmarth, 1989. Reynolds number effects on the structure of a turbulent channel flow. *J. Fluid Mechanics*, 204: 57-95.

24. Piomelli, U., 1993. High Reynolds number calculations using the dynamic subgrid-scale stess model. *Physics of Fluids A*, 5: 1484-1490.

25. Najjar, F. M. and D. K. Tafti, 1997. Evaluation of the dynamic subgrid-scale stress model in finite-difference LES; effects of grid resolution and inhomogeneous test filtering. Proceedings of the First AFOSR International Conference on Direct Numerical Simulation and Large Eddy Simulation.